Civil Engineering

# Flow characteristics downstream stepped back weir with bed water jets

M.M. Ibrahim [a],*, Mahmoud A. Refaie [a], Ahmed M. Ibraheem [b]

[a] Shoubra Faculty of Engineering, Benha University, PO Box 11629, Shoubra, Egypt
[b] Hydraulics Research Institute, National Water Research Center, Cairo, Egypt

## ARTICLE INFO

## ABSTRACT

The development of hydraulic jump downstream weirs creates local scour that may affect the overall stability of the structure or even cause complete failure. In this study, an experimental work was carried out to present a new technique using bed water jets installed to the classical smooth apron to present stilling basin with specific characteristics motivated to dissipate the hydraulic jump energy. Five rows of bed water jets were implemented to explore their presence on the energy dissipation efficiency, the hydraulic jump characteristics, and the vertical and longitudinal flow velocity distributions downstream of the weir apron toe under skimming flow regime in stepped back weirs. Three different arrangements of bed water jets were used in addition to the reference case of a non-jetted system. The sum of jets discharge from the three activated rows were constant of 12 Lit/s. The tested total discharges were 120, 150, and 180 Lit/s. Each discharge was examined with three tailwater depths of 20, 25, and 30 cm. Initial Froude numbers ranging from 1.15 to 4.99 were applied under relative jet discharges ranging from 0% to 10% of the total discharge. The results showed that by activating the middle 3 rows, the average hydraulic jump energy dissipation efficiency can be improved by up to 70.8%, and the average jump lengths can be decreased by up to 48% compared to the non-jetted system. Using stepped back weir increased the energy dissipation efficiency and decreased the jump length by about 40% and 31%, respectively compared to 1:2 sloped back weir for similar flow conditions. Finally, possible future research directions were suggested.

© 2021 THE AUTHORS. Published by Elsevier BV on behalf of Faculty of Engineering, Ain Shams University. This is an open access article under the CC BY-NC-ND license (http://creativecommons.org/licenses/by-nc-nd/4.0/).

The hydraulic jump dissipates energy downstream of the weir, the efficiency of energy dissipation can be sufficiently increased using bed water jets and stepped back weirs.

## 1. Introduction

Weirs are widely used in open channels for flow measurements and to control the water levels. These structures are usually associated with a noticeable change in flow energy dissipation by the formation of a downstream hydraulic jump which endangers the stability of these structures [1]. The hydraulic jump characteristics were studied by Long et al., [2]. The study presented experimental and numerical investigations on the effect of wall friction on the water level downstream of the hydraulic jump. Chanson and Toombes [3] experimentally studied the submerged hydraulic jump by calculating the water surface profile and flow velocity and comparing the experimental and the calculated measurements. Hossein et al., [4] studied the energy dissipation over stepped spillway under skimming flow regime. The results explored that the energy scattering is decreased as the relative discharges increased. The studies of flow over a stepped spillway are categorized into two main groups; the first is focused on the water surface profile and energy dissipation, while the second focuses on the effect of changing slope on energy dissipation [5]. Computational fluid dynamics (CFD) modeling is applied to solve the equations for the conservation of the mass, momentum, and energy of the fluid flow. Javan and Eghbalzadeh [6] simulated submerged hydraulic jumps using a 2D k-ε turbulence model and a Lagrangian moving grid method for free-surface tracking. Jesudhas et al., [7] analytically investigated 3D submerged hydraulic jumps by utilizing the volume of fluid (VOF) method combined with a detached eddy simulation, and the results were compared to the experimental observations. The investigations confirmed the model's ability to predict accurately the characteristics of a submerged hydraulic jump. The (VOF) method was also applied by Helal et al., [8] to

---

* Corresponding author.

Peer review under responsibility of Ain Shams University.

**Nomenclature**

| | | | |
|---|---|---|---|
| B | Flume width [m] | $U_m$ | Maximum flow velocity at any cross section downstream of the weir apron [m/s] |
| $d_{50}$ | Median particle diameter [mm] | | |
| $D_j$ | Jet diameter [cm] | X | Longitudinal distance measured from the weir toe to the middle-activated row of jets for a given group [m] |
| $D_{JL}$ | Distance between jet lines [cm] | | |
| $E_1$ | Initial specific energy [m] | y | Flow depth at a given point [cm] |
| $E_2$ | Sequent specific energy [m] | $y_{up}$ | Upstream flow depth [cm] |
| g | Gravitational acceleration [m/s$^2$] | $y_1$ | Hydraulic jump initial flow depth [cm] |
| $L_b$ | Basin length [m] | $y_2$ | Hydraulic jump sequent depth [cm] |
| $L_j$ | Hydraulic jump length [m] | $y_t$ | Tailwater depth [cm] |
| N | Number of steps [–] | $\rho$ | Water density of the flow [kg/m$^3$] |
| $Q_{sw}$ | Flow discharge over stepped back weir [Lit/s] | $\mu$ | Water dynamic viscosity [kg/m.s] |
| $Q_j$ | Flow discharge from floor jets [Lit/s] | $\sigma$ | Water surface tension [N/m] |
| $Q_t$ | Total flow discharge [Lit/s] | $\eta$ | Energy dissipation efficiency [–] |
| $S_h$ | Step height [m] | $F_r$ | Froude number [–] |
| $S_w$ | Step width [m] | $R_e$ | Reynolds number [–] |
| U | Mean longitudinal flow velocity at a given point [m/s] | $W_e$ | Weber number [–] |
| $U_1$ | Hydraulic jump initial flow velocity [m/s] | | |
| $U_2$ | Hydraulic jump sequent velocity [m/s] | | |

compute the characteristics of the submerged jumps. In modeling the turbulence stresses, k-ω shear stress transport (SST) and Reynolds averaged Navier-Stokes (RANS) equations are employed. The modeled velocity profiles displayed a good agreement with the corresponding experimental measurements. The simulated results detailed that the implementation of bed water jets enhanced the efficiency of the submerged hydraulic jumps by up to 85.4% and decreased the submerged jump lengths by up to 59% compared to the non-jetted system.

Many researchers have also applied computational software to explore the hydraulic jump characteristics downstream of hydraulic structures. Researchers have used sills, chutes, and baffle blocks to reduce the jump length and consequently shorten the basin length required for a designed discharge [9–11].

Experimental studies were also employed to simulate the flow pattern downstream of stepped weirs in addition to the evaluation of the effect of different bed configurations on scour and silting. Amany et al., [12] experimentally concluded that using a stepped spillway reduced the relative scour depth and increased the relative energy loss in comparison to the back sloped weir. Ahmed [13] carried out laboratory studies to explore the effect of 5 rows of bed water jets on the flow characteristics downstream of weirs with a sloped back. The results indicated that the stilling basin design using the last three jet rows gave the lowest velocity distribution and the highest energy dissipation. Consequently, this is considered the optimum design with respect to the stability of the bed material.

Zhang and Chanson examined the skimming air–water properties on a stepped spillway for varies geometries of steps [14]. The outcomes determined that the chamfered steps prompted an increase in mean velocity gradient, consequently decreased the energy dissipation.

Al-Fawzy et al., [15] studied the effect of 3 stepped gabion weir on dissipated energy of flow. The results showed that the energy dissipation was directly proportional to the discharge, and inversely proportional to the ratio of length of the third step to total length of the weir. Chaiyuth et al., [16] experimentally studied the hydraulics of flow through and over gabion-stepped weirs. The main flow through the voids between the filled stones and the overflow on the gabions were observed. The energy loss ratios in the gabion-stepped weirs were found greater than those in the corresponding horizontal stepped weirs. Stone size and shape have

insignificant influence on the energy loss and flow velocity compared to the noticeable effect of the weir slope. Azza et al., [17] tested 27 stepped weir models with 3 different heights, slopes and number of steps. The study demonstrated that the energy dissipation increased by the increase of the hydraulic jump length, the weir slope, the number of steps, and the decrease of the weir height. The optimum design for energy dissipation is that have greater slope, lower height, and greater steps number. Stefan and Hubert [18] conducted a laboratory study on a moderate slope-stepped weir (1 V:2H) and five stepped configurations. The outcomes indicated that the rate of energy dissipation was similar for uniform and non-uniform stepped configurations. However, the non-uniform stepped configurations induced some flow instabilities in the case of small flow rates. Jean and Bassam [19] experimentally studied the hydraulics of Ogee-profile stepped spillways to examine their ability as a suggested alternative to smooth-back spillways from the point of view of reducing the downstream energy and the hydraulic jump length. The study concluded that the number of steps is the overbearing factor in expending flow kinetic energy and therefore, reducing the length of the downstream forming hydraulic jump. Changing the slope of steps in stepped back weir is applicable to increase energy dissipation. Ali and Yousif [20] used 3 physical models to investigate the energy dissipation due to the installation of stepped back weir with steps of transverse slope along step in a zigzag way. The results showed that steps having transverse slope gave 14% higher energy dissipation compared to the classical stepped weir model with flat steps. Shicheng and James [21] numerically explored the effect of step slope upward and downward along the flow direction on the energy dissipation. The results explored that the shifting from a downward to an upward layout exhibited higher energy dissipation efficiency. Ghaderi et al. [22] carried out numerical simulations on a spillway with trapezoidal labyrinth-shaped steps (TLS). The study exhibited that the (TLS) increased the energy dissipation up to 17%. Considering the two-phase air–water flow along the spillway; Zongshi et al., [23] used Computational Fluid Dynamics (CFD) to investigate air–water two-phase flow on stepped spillway behind X-shaped flaring gate piers under very high unit discharge. The results concluded that the involved models can predict the air concentration near the steps. The cavitation index at the stepped surface was below the threshold value, and the air concentration was insufficient under high unit discharges.

The two-phase flow over two types of step-pool spillway was investigated by Nikseresht et al., [24]. The study used numerical simulation of two-phase flow carried out on two types of step-spillway with various slopes. The study revealed that the mixture model with the Reynolds Stress turbulence Model (RSM) was suitable for simulation of two-phase flow over spillways.

Due to the significance of the stepped back weir as a water control structure, specifically in energy dissipation, this study performs laboratory experiments using different bed water jets arrangements installed at the apron of stepped back weir. In addition, the variations of hydraulic jump characteristics and velocity distributions downstream of the weir apron toe with different hydraulic conditions are presented. Regarding the adequacy of the discussed technique for practical application, an independent study should be presented to include the contribution of electromechanical specialists for estimation of field pump capacity and the head loss in the feeding system. Moreover, a significant contribution from project management specialists to prepare a financial study to identify how far the economics of the presented technique.

## 2. Theoretical background

The bed water jets downstream of stepped back weir that affect the hydraulic jump characteristics and velocity distributions downstream of the weir apron considered in this study are shown in Fig. 1 and are as follows:

$B$, the flume width; $y_t$, the tailwater depth; $U$, the mean longitudinal velocity; $U_1$, the hydraulic jump initial velocity; $U_2$, the hydraulic jump sequent velocity; $y_{up}$, the upstream flow depth; $y_1$, the hydraulic jump initial water depth; $y_2$, the hydraulic jump sequent depth; $g$, the gravitational acceleration; $\rho$, the water density of the flow; $\mu$, the water dynamic viscosity; $\sigma$, surface tension,

$Q_{sw}$ the discharge over stepped back weir; $Q_j$, the discharge from bed jets; $Q_t$, the total discharge at the tail of the channel, where $(Q_t = Q_{sw} + Q_j)$; $L_j$, the hydraulic jump length; $\eta$, the energy dissipation efficiency; $L_b$, the basin length; $S_h$, the step height; $S_w$, the step width; $N$, number of steps; $D_{JL}$, distance between jet lines; $D_J$, jet diameter; $X$, the longitudinal distance measured from the weir toe to the middle activated row of jets for a given group.

$$\eta = \frac{E_1 - E_2}{E_1} \tag{1}$$

where $E_1$ is the initial specific energy, and $E_2$ is the sequent specific energy.

$$E_1 = y_1 + \frac{U_1^2}{2g} \tag{2}$$

$$E_2 = y_2 + \frac{U_2^2}{2g} \tag{3}$$

$$\varphi(B, y_t, S_h, S_w, N, L_b, L_j, D_j, D_{JL}, Q_{sw}, Q_j, Q_t, U, U_1, U_2, y_1, y_2, \mu, L_j, \eta, \rho, X, \sigma)$$
$$= 0 \tag{4}$$

Through this study, B, $S_h$, $S_w$, N, $L_b$, $D_j$, $D_{JL}$ are kept constant; so they are unconsidered from Equation (4).

Based on dimensional analysis using Buckingham's theorem, the following dimensionless groups can be obtained:

$$f\left(\frac{Q_j}{Q_t}, \frac{L_j}{y_1}, F_r = \frac{U}{\sqrt{gy}}, \frac{X}{y_1}, \eta, R_e = \frac{\rho Q_t}{B\mu}, W_e = \frac{\rho U^2 B}{\sigma}, \frac{B}{y_1}, \frac{S_h}{y_1}, \frac{S_w}{y_1}, N, \frac{L_b}{y_1}, \frac{D_J}{y_1}, \frac{D_{JL}}{y_1}\right)$$
$$= 0 \tag{5}$$
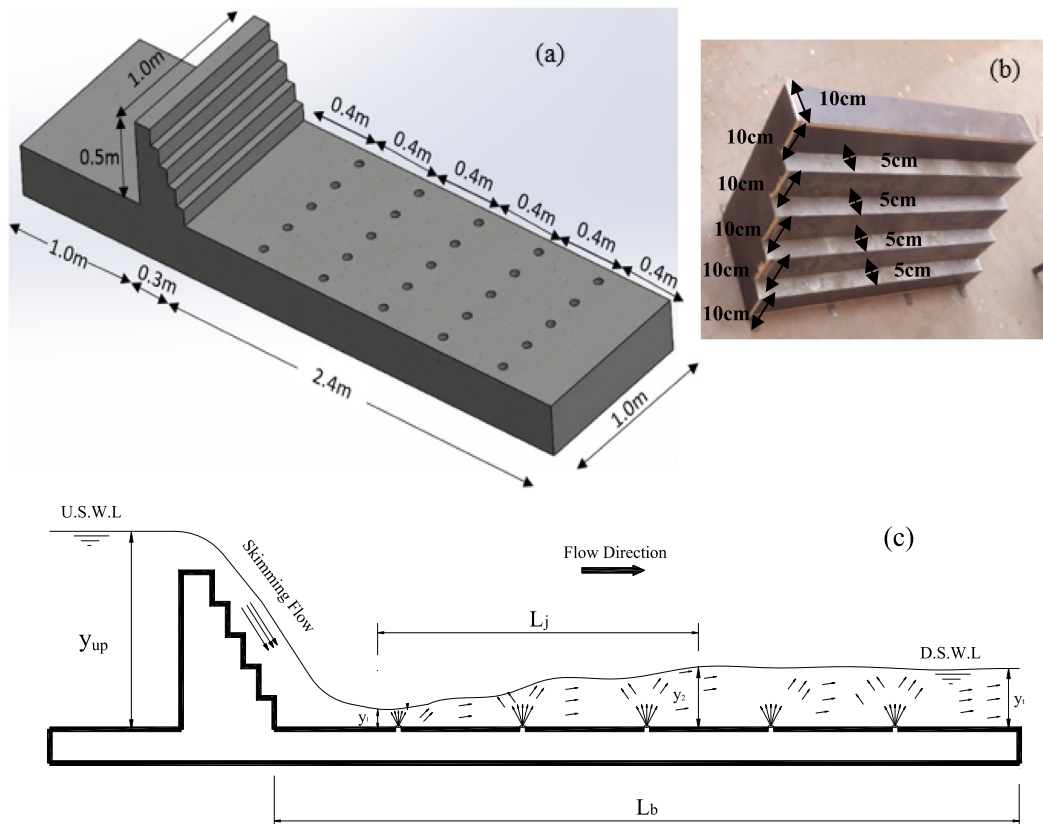


**Fig. 1.** Stepped Back Weir: (a) A Sketch with Bed Water Jets; (b) Actual Model; (c) Flow Pattern.

where $F_r$ is the Froude number calculated at the section where $y$ and $U$ are measured, and $R_e$ and $W_e$ are the Reynolds and Weber numbers respectively which can be neglected due to the insignificant influence since the flow is in open channel and the head over the weir more than 3 cm. Therefore, Equation (5) can be summarized to:

$$f\left(\frac{Q_j}{Q_t}, \frac{L_j}{y_1}, F_r = \frac{U}{\sqrt{gy}}, \frac{X}{y_1}, \eta\right) = 0 \tag{6}$$

## 3. Experimental setup and procedures

### 3.1. Experimental setup

The experimental work was conducted in the hydraulic laboratory at the Hydraulics Research Institute, (HRI), Egypt using a flume 26.0 m long, 1.0 m wide and 1.20 m deep. The side walls along the flume length are made of glass with steel frames, to allow visual investigation of the flow patterns. The horizontal bottom floor of the flume is made of concrete. The tailwater depth; $y_t$ is controlled by a tailgate at the downstream end of the flume. The water is supplied to the flume from a constant head tank, which is fed by a centrifugal pump with a total discharge of 300 Lit/s. The flume inlet consists of a masonry basin of 3.0 m width, 3.0 m length and 2.5 m depth. The water passes across a screen box filled with large gravel followed by another screen box filled with 2 in.-diameter plastic pipes at the inlet to dissipate the energy and scatter any excessive turbulence. The flume exit consists of a basin that starts directly after the flume end following the tailgate. Fig. 2 shows details of the tested flume. The hydraulic model structure of the stepped back weir is made of wood and installed at

10.7 m distance downstream the flume inlet. The weir height is 0.5 m, the crest width is 0.1 m, and the weir back have 4 steps each step is 0.05 m wide and 0.10 m high. The total width of the weir is 1.0 m. The weir model dimensions was selected after many trial tests, as the more increase of weir height led to flow overtopping in case of $Q_t$ = 180 Lit/s, while the short weir height did not develop considerable hydraulic jump. The stilling basin is a horizontal 3.70 m long basin, divided into three parts; 1.0 m upstream of the weir, 0.30 m weir, and a weir apron 2.4 m downstream of the weir. Five rows of bed water jets are installed and levelled in the weir apron each row has five 0.9 cm diameter jets. The jets are pointed vertically upward without inclination angle to the apron. The first row is located at $\frac{1}{6}L_b$ from the weir toe. Also, the distance between jet rows is $\frac{1}{6}L_b$. Fig. 1 shows the detailed components of the tested model. The distance downstream of the weir apron is filled with a layer of 25 cm deep sand of $d_{50}$ = 0.423 mm levelled to the weir apron.

### 3.2. Experimental program

Thirty-six experimental tests were performed utilizing 3 total discharges, $Q_t$ of 120, 150, and 180 Lit/s., 3 scenarios for jet operations arrangements, and 3 tailwater depths, $y_t$ of 20, 25, and 30 cm. The runs are categorized by the jets arrangement into 4 cases. The case (A) is viewed as the base case of non-jetted system; where the bed water jets are deactivated. In cases (B), (C), and (D), the bed water jets are enabled where only three of the five lines are activated regardless of their arrangement to give a steady jets discharge of $Q_j$ = 12 Lit/s for the three jet lines. The operation of bed water jets are as indicated by 3 scenarios; where the initiated jet rows are the first three (i.e. No. 1, 2, and 3) to present case (B),
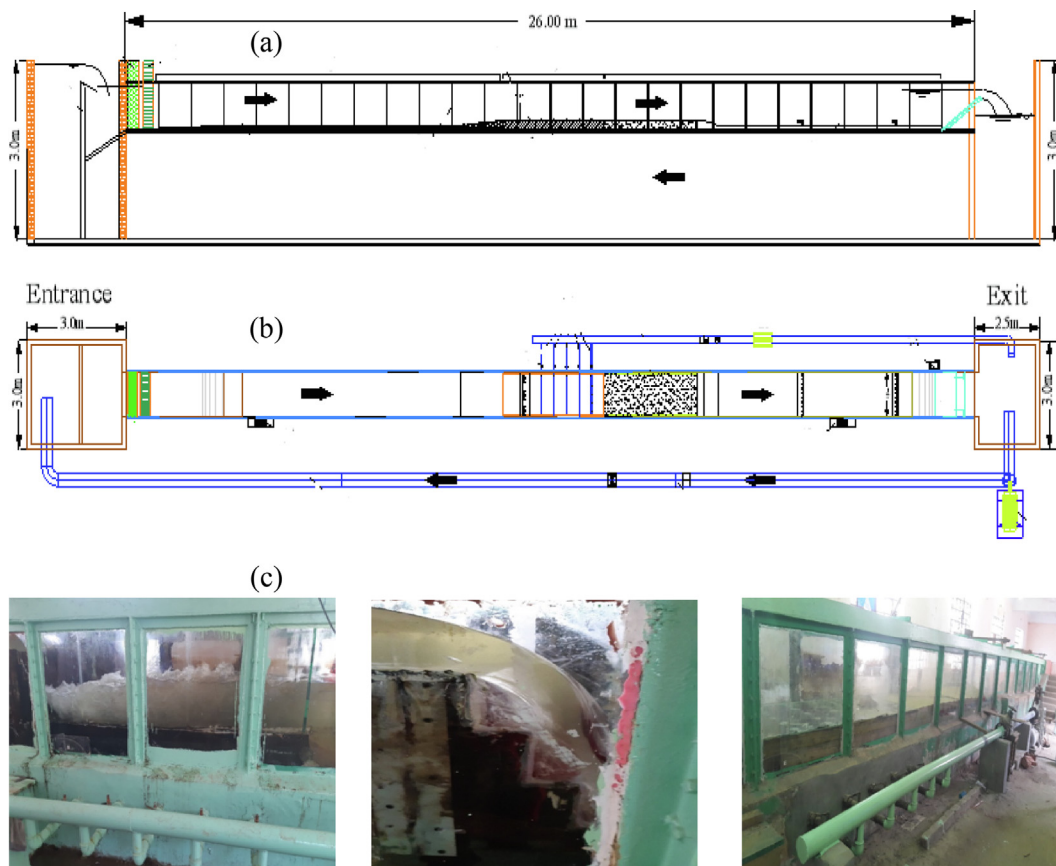


**Fig. 2.** The Experimental Model: (a) Elevation; (b) Plan; (c) Perspectives.

or the middle three (i.e. No.2, 3, and 4) to present case (C), or the last three jet lines (i.e. No. 3, 4, and 5) to present case (D); Fig. 1. The experimental test program is summarized in Table 1.

### 3.3. Experimental procedures

The flume tailgate was totally closed, the main pump was switched-on to fill the flume with water in very low rate to a certain water level. The supplied discharge was measured by an ultrasonic flowmeter with an accuracy of ±1%. A secondary pump was used for adjusting the bed water jet flow discharges through a 4-inch pipeline, which was measured by an electromagnetic flowmeter with an accuracy of ±1% installed on the pipeline. Each row of bed jets has a control valve at its inlet used to control the operation of the bed water jets rows. The downstream flow depths were adjusted to obtain the required test conditions. After reaching steady state, the upstream flow depth, $y_{up}$; the initial flow depth of the hydraulic jump, $y_1$; the length of hydraulic jump, $L_j$; the flow depths along stilling basin each 20 cm starting from the weir toe were recorded. The velocity, $U$ was measured using an Electromagnetic Current-meter type E.M.S. (manufactured by Delft Hydraulics) with an accuracy of ±0.2%. The center line velocity was measured at 6 locations started by the weir apron toe and extended to 5 m along the flow direction. The distance between locations was constant of 1 m. At each location, the vertical velocity was recorded at 0.2, 0.4, 0.6, 0.8, and 0.9 of the measured flow depths, $y$. The experimental measurements were recorded after six hours. The selected run time duration were adopted according to the appreciable movement of bed material regardless the stability of hydraulic jump that consumed time less than the selected run duration. The six hours were sufficient enough where the quasi-equilibrium state was initiated and the formed scour hole shape was unchanged with time. Finally, the tailgate was tilted to drain the flume. The previous steps were repeated for each arrangement listed in Table 1.

### 3.4. The scale effect

Underscoring the experimental scale effects, there are few unconsidered parameters in the current investigations because of their minor influence which are as the following:

The head loss in the nozzles pipeline might be ignored because of its short length which is 1.2 m; the air entertainment and transport capacity of a high-speed model flow in weir steps and due to the bed water jet interaction with the main flow; the friction of flow with the glass flume side walls; viscous and surface tension forces presented in terms of Reynolds and Weber numbers due to their insignificant effect since the flow is in open channel.

## 4. Results and discussions

The recorded experimental results are analyzed and discussed in this section to evaluate using bed water jets downstream of a stepped back weir under skimming flow regime and the effect of jets different arrangements on the energy dissipation efficiency, the hydraulic jump characteristics, the vertical velocity distribution and the water surface profiles.

**Table 1**
Experimental Test Program.

| Arrangement No. | Flow Conditions | | | | Activated Jet Rows | | |
|---|---|---|---|---|---|---|---|
| | Test No. | $Q_t$ (Lit/s) | $Q_j$ (Lit/s) | $y_t$ (cm) | Jet Row No. | Jet row distance downstream of weir (m) | $\sum Q_j/Q_t$ (%) |
| A | 1 | 120 | 0 | 20 | No Jets | | |
| | 2 | | | 25 | | | |
| | 3 | | | 30 | | | |
| | 4 | 150 | | 20 | | | |
| | 5 | | | 25 | | | |
| | 6 | | | 30 | | | |
| | 7 | 180 | | 20 | | | |
| | 8 | | | 25 | | | |
| | 9 | | | 30 | | | |
| B | 10 | 120 | 12 | 20 | 1, 2, and 3 | 0.4, 0.8, and 1.2 m | 10 |
| | 11 | | | 25 | | | |
| | 12 | | | 30 | | | |
| | 13 | 150 | | 20 | | | 8 |
| | 14 | | | 25 | | | |
| | 15 | | | 30 | | | |
| | 16 | 180 | | 20 | | | 6.67 |
| | 17 | | | 25 | | | |
| | 18 | | | 30 | | | |
| C | 19 | 120 | 12 | 20 | 2, 3, and 4 | 0.8, 1.2, and 1.6 m | 10 |
| | 20 | | | 25 | | | |
| | 21 | | | 30 | | | |
| | 22 | 150 | | 20 | | | 8 |
| | 23 | | | 25 | | | |
| | 24 | | | 30 | | | |
| | 25 | 180 | | 20 | | | 6.67 |
| | 26 | | | 25 | | | |
| | 27 | | | 30 | | | |
| D | 28 | 120 | 12 | 20 | 3, 4, and 5 | 1.2, 1.6, and 2.0 m | 10 |
| | 29 | | | 25 | | | |
| | 30 | | | 30 | | | |
| | 31 | 150 | | 20 | | | 8 |
| | 32 | | | 25 | | | |
| | 33 | | | 30 | | | |
| | 34 | 180 | | 20 | | | 6.67 |
| | 35 | | | 25 | | | |
| | 36 | | | 30 | | | |

### 4.1. The energy dissipation efficiency

Applying dimensional analysis tool to the parameters affecting these phenomena, the dimensionless parameters listed in Equation (6) can be used to study the energy dissipation at the hydraulic jump. The relationship between Froude number at the initial depth, $F_{r1}$ and the jump energy dissipation efficiency, $\eta$ for different bed water jets arrangements is shown in Fig. 3, for $Q_t$ = 180 Lit/s and $y_t$ = 20 cm. It is observed that when $F_{r1}$ increases the efficiency of bed water jets, $\eta$ decreases regardless to the bed water jets arrangement. These findings are in good agreement with Helal et al., [8] and Ahmed [13] results. However, the jets installation remarkably increased the energy dissipation efficiency compared to the non-jetted system of case (A). Considering the jet arrangements, it is noticed that the max energy dissipation efficiency is reported for the case (C). However, the lowest values are presented for case (A) at constant Froude number. The increased percentage of the energy dissipation efficiency reached with an average of 70.8% for case (C) compared to the non-jetted system in case (A). Therefore, the case (C) gave the optimum bed water jets arrangement in terms of the energy dissipation. That is because the action

of bed water jets in case (C) is pointed to a specific region in the generated downstream hydraulic jump which is the jump roller leading to consequential dissipation of the flow energy. On the other hand, using stepped back weir increased the energy dissipation efficiency, $\eta$ compared to sloped back weir by 1:2 presented by Ahmed [13] under similar experimental flow conditions. Fig. 4 shows the relation between $F_{r1}$ and $\eta$ for the stepped and sloped back weir. It is underscored that $\eta$ has greater values using stepped back weir than the sloped back ones for the same Froude number, $F_{r1}$ value by an average of 40%. That is referred to the action of the steps; where the flow scattered some of its energy by crashing with the weir steps. These findings are consistent with Amany et al., [12] outcomes.

### 4.2. The hydraulic jump characteristics

The variation of the dimensionless hydraulic jump length, $L_j/y_1$ with the different bed water jets arrangement are also studied and presented in Fig. 5. It was found that the dimensionless jump length, $L_j/y_1$ is increased with the increase of the Froude number upstream of the hydraulic jump, $F_{r1}$ for any mode of jet operations
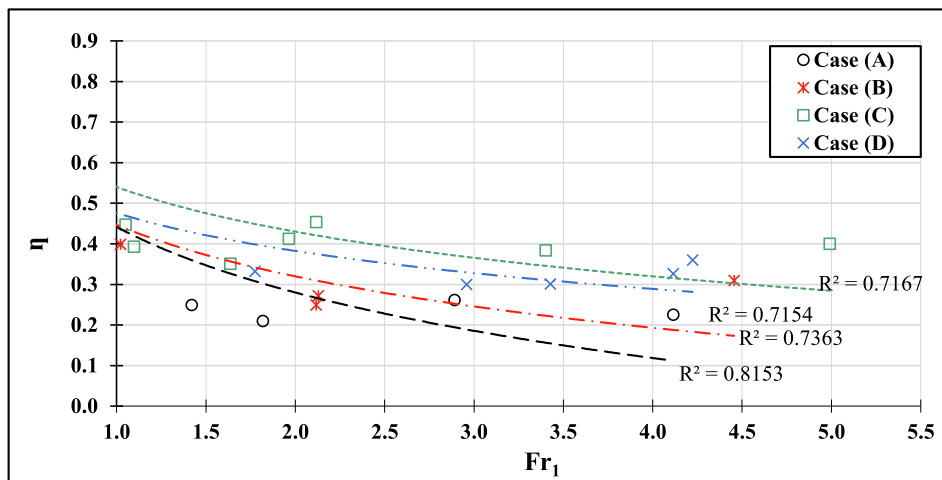


**Fig. 3.** Energy Dissipation Efficiency for different Bed Water Jets Arrangements.
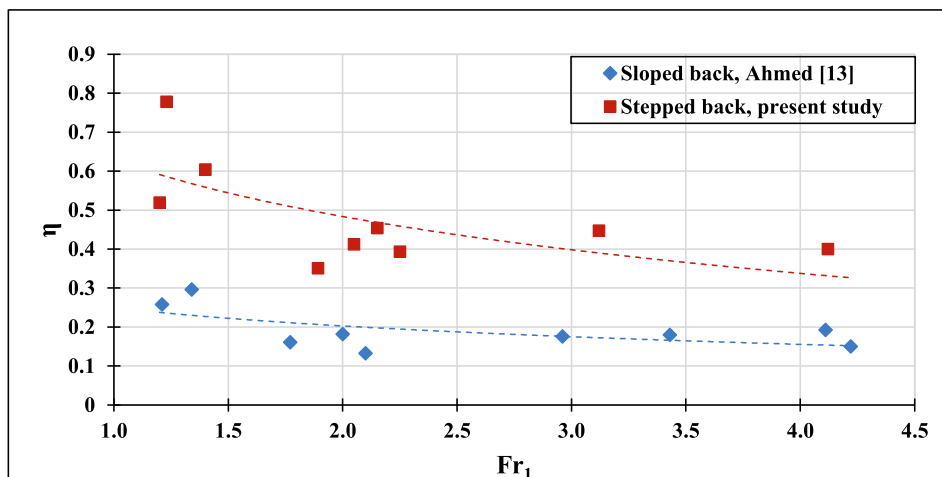


**Fig. 4.** Energy Dissipation Efficiency for the Elaborated Stepped Back Weir and Sloped Back Weir; Ahmed [13] at $\sum Q_j/Q_t$ = 6.67.
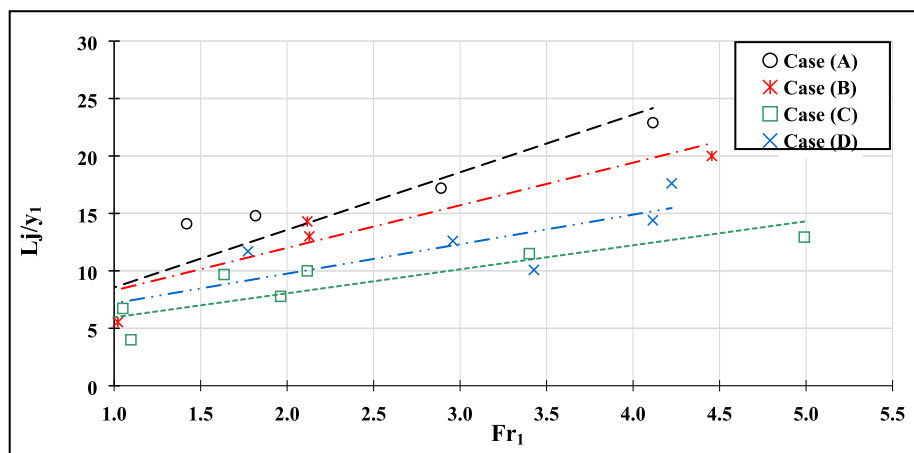
**Fig. 5.** Dimensionless Hydraulic Jump Lengths for different Bed Water Jets Arrangements.

due to the noticeable increase in jump turbulences. The curves trend is consistent with Helal el al., [8].

Fig. 5 shows that $L_j/y_1$ decreases by using bed water jets compared to the non-jetted case (A) with an average of 74%. Also, the case (C) gave the shortest dimensionless jump lengths compared to other tested cases of jets arrangements because of the same reasons discussed earlier in Section 4.1 regarding the location of jets with respect to the jump roller.

Fig. 6 shows the influence of the stepped back weir on the hydraulic jump characteristics compared to the sloped back weir. The figure shows the relationship between $F_{r1}$ and $L_j/y_1$ for the present measurements and the corresponding values reported by Ahmed [13] for the similar flow conditions. The figure demonstrated that the dimensionless hydraulic jump length, $L_j/y_1$ are found to be smaller by an average of 31% for the stepped back weir compared to the sloped back weir. That clearly shows the merits of the stepped back weir in decreasing the jump length which is in a good agreement with Jean and Bassam [18].

Figs. 7 and 8 explore the effect of tailwater depth, $y_t$ and total discharge, $Q_t$ on the dimensionless hydraulic jump length, $L_j/y_1$. Fig. 7 is plotted for $Q_t$ = 180 Lit/s under different tailwater depths while Fig. 8 is presented for $y_t$ = 20 cm for various discharges. These figures indicated that the $L_j/y_1$ decreases with the increase of tailwater depth, $y_t$ and the decrease of total discharge, $Q_t$ for the tested

flow conditions. The reasons are focused on the hydraulic jump initial velocity, $U_1$ and typically the corresponding upstream hydraulic jump Froude number, $F_{r1}$. Where these parameters are inversely related to the tailwater depth, $y_t$ and directly to the total discharge, $Q_t$ which is confirming the conclusions explored of Fig. 5.

Taking into account the influence of the jets arrangements, Figs. 7 and 8 and Table 2 show that the presence of bed water jets regardless of their arrangements decreased the dimensionless hydraulic jump length, $L_j/y_1$ compared to the non-jetted case (A). However, the case (C) presents the optimum water jets arrangement, where the maximum reduction in $L_j/y_1$ is recorded for the tested tailwater depths.

### 4.3. The velocity distribution downstream of the weir apron

Fig. 9 presents a survey of the vertical velocity distribution for $Q$ = 180 Lit/s and $y_t$ = 20 cm at the weir apron toe. Fig. 9 illustrates that the maximum velocity ratios, $U/U_1$ are 0.364, 0.302, 0.205, and 0.243 for cases (A), (B), (C), and (D) respectively. Hence, the velocity ratio is decreased by 17.03, 43.68, and 33.24%, for cases (B), (C) and (D), respectively compared to case (A). Thus, using case (C) gives the optimum bed water jet arrangement that decreasing the velocities at the weir apron. It should be noticed that no negative velocities are recorded because the length of jump roller ended
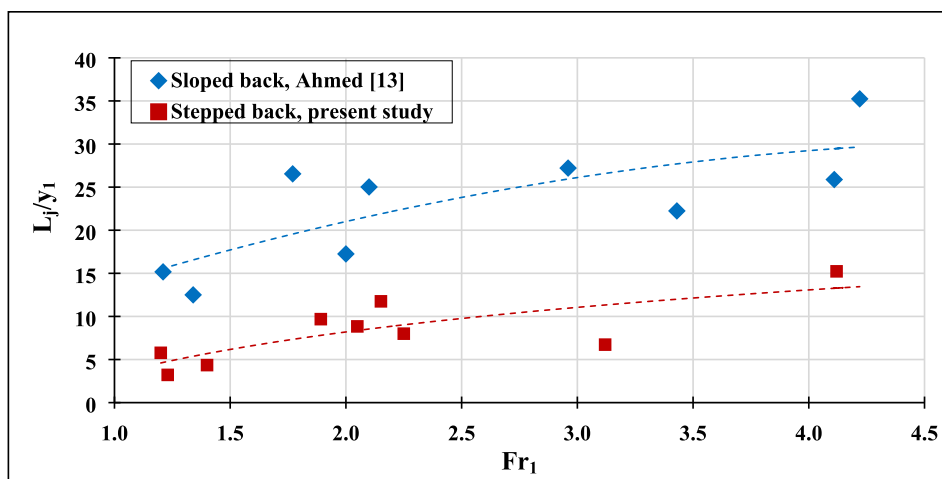


**Fig. 6.** Comparison between the Dimensionless Hydraulic Jump Lengths for the Elaborated Stepped Back Weir and Sloped Back Weir; Ahmed [13] at $\sum Q_j/Q_t$ = 6.67.
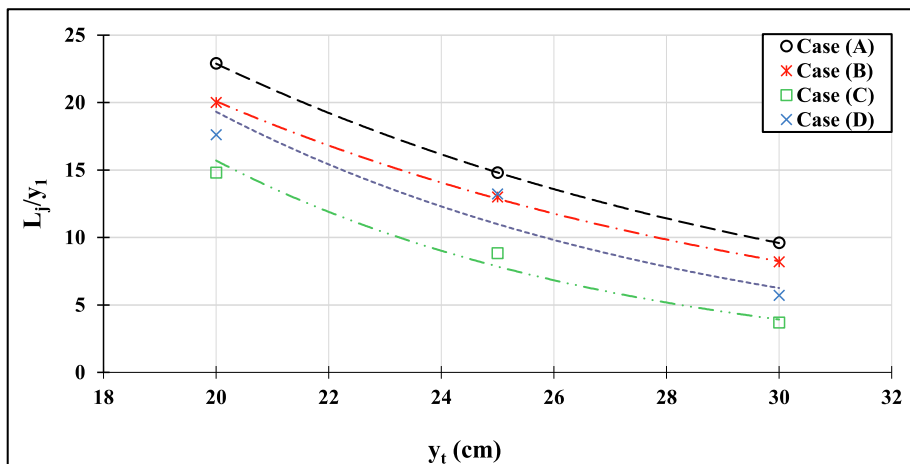
**Fig. 7.** Dimensionless Hydraulic Jump Lengths with the Tailwater Depths for different Bed Water Jets Arrangements.
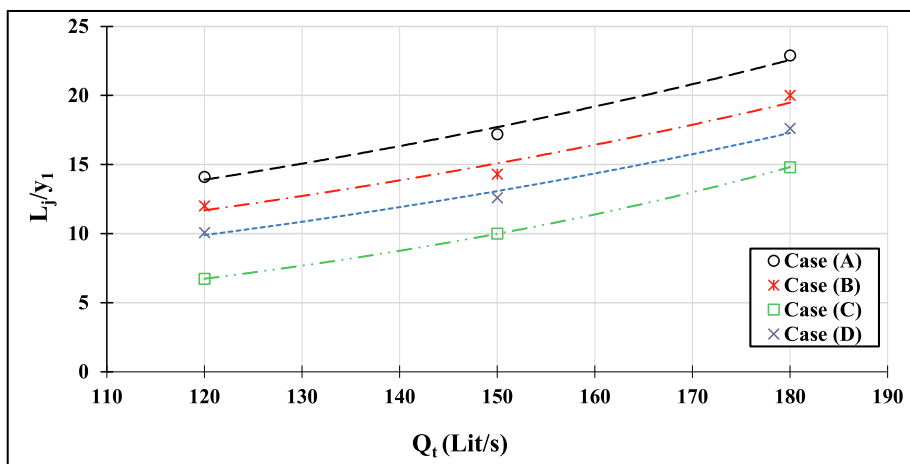


**Fig. 8.** Dimensionless Hydraulic Jump Lengths with the Total Discharge for different Bed Water Jets Arrangements.

**Table 2**
Effect of Bed Jets Arrangement Compared to Case (A).

| Jets Arrangements $y_t$ (cm) | % Reduction in $L_j/y_1$ for $Q_t$ = 180 Lit/s | | |
|---|---|---|---|
| | Case (B) | Case (C) | Case (D) |
| 20 | 12.66 | 35.37 | 23.10 |
| 25 | 12.16 | 40.27 | 10.61 |
| 30 | 14.58 | 61.46 | 40.63 |

before the weir apron toe where the velocity measurements took place. Hence most turbulences by the jump action is vanished.

The velocity distributions in the longitudinal direction downstream of the weir apron toe are explored for the different bed water jets arrangements. The maximum flow velocity values at 6 different sections and bed water jets arrangement cases corresponding to $Q$ = 180 Lit/s and $y_t$ = 20 cm are recorded and tabulated
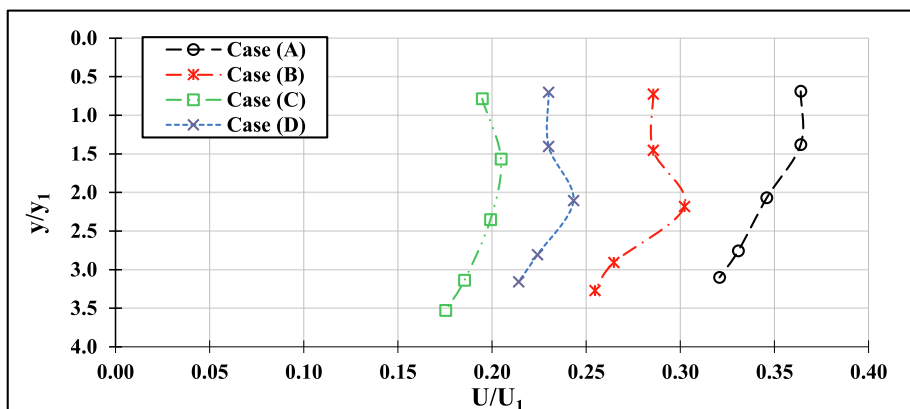


**Fig. 9.** Vertical Velocity Distributions at the Weir Apron Toe.

**Table 3**
Maximum Vertical Velocity at different Longitudinal Sections.

| Section | Maximum velocity in the vertical distribution, $U_m$ (m/s) for different cases | | | |
|---|---|---|---|---|
| | Case A | Case B | Case C | Case D |
| 0 | 1.050 | 1.202 | 0.981 | 1.055 |
| 1 | 0.774 | 0.965 | 0.665 | 0.864 |
| 2 | 0.827 | 0.679 | 0.775 | 0.830 |
| 3 | 0.765 | 0.686 | 0.695 | 0.744 |
| 4 | 0.699 | 0.71 | 0.655 | 0.798 |
| 5 | 0.775 | 0.765 | 0.721 | 0.867 |
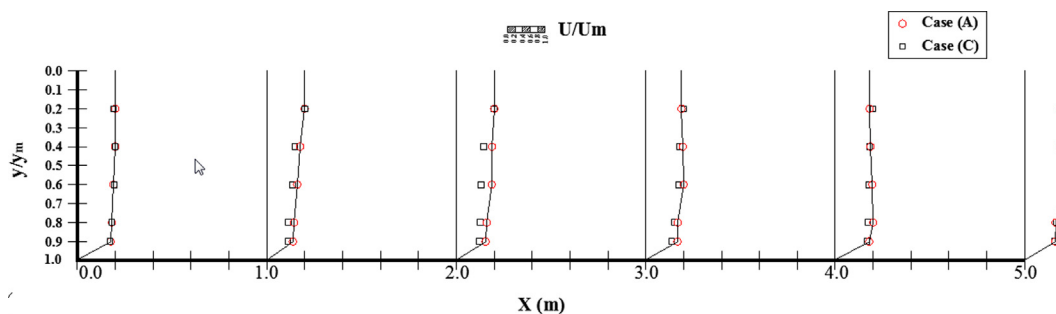


**Fig. 10.** Vertical Velocity Distributions at different Sections along the Flume Length Downstream the Weir Apron Toe.

in Table 3. The cross sections are 1 m a part started from weir apron toe and extended for 5 m along the flow direction. The table illustrates that the maximum flow velocity values for case (C) are minimized for all sections with an average of 9.07%.

For thoroughly investigations regarding the flow velocity distributions along the channel length; Fig. 10 is presented. The figure gives a comparison between case (A) and case (C) regarding the vertical velocity component $U$ at longitudinal distance $X$ from the weir apron toe at the sections described in Table 3. The figure is plotted for $Q = 180$ Lit/s and $y_t = 20$ cm; where the most critical case regarding the flow velocities is occurred. For the tested cases, it was found that the flow velocity values are decreased through the five sections next to the weir apron toe due to the development of scouring hole in the bed material at the downstream, where the flow depth is increased. Then, the flow velocities are increased again by the end of the souring region due to the decreasing of flow depth, referring to the initiation of sedimentation zone. The figure

confirmed the findings of Fig. 9 and Table 3, where the velocity values are noticeably decreased for case (C) compared to case (A) at different cross sections.

Fig. 11 explores the performance of the maximum longitudinal flow velocity, $U_m$ along the channel length for different scenarios of jets arrangement ($Q = 180$ Lit/s and $y_t = 20$ cm). The figure shows the ratio of the maximum longitudinal flow velocity to the initial flow velocity ratio, $U_m/U_1$ at different longitudinal sections, $X/y_1$ starting from the weir apron toe. This figure demonstrates that as the $X/y_1$ is increased, the $U_m/U_1$ is decreased. That is reasoned by the hydraulic jump influences are minimized as the flow shifted far from the weir apron toe and as a result the $U_m$ is decreased. The outcome curves trend is consistent with Helal el al., [8]. Considering the jets arrangement, the figure shows that case (C) gives the smallest values of $U_m/U_1$ along the channel length at the six allocated longitudinal sections. These findings confirming the advantage of case (C) in minimizing the flow velocity distribution.
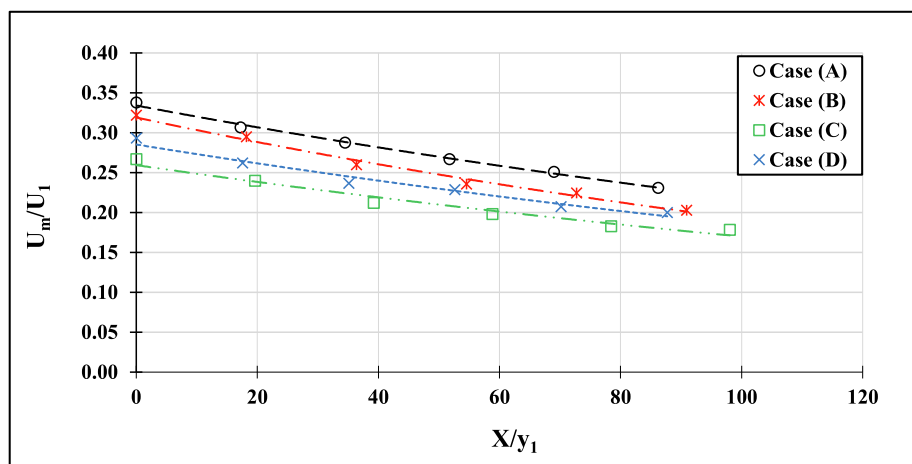


**Fig. 11.** Maximum Longitudinal Vertical Flow Velocity ratio to Initial Flow Velocity at different Longitudinal Sections.
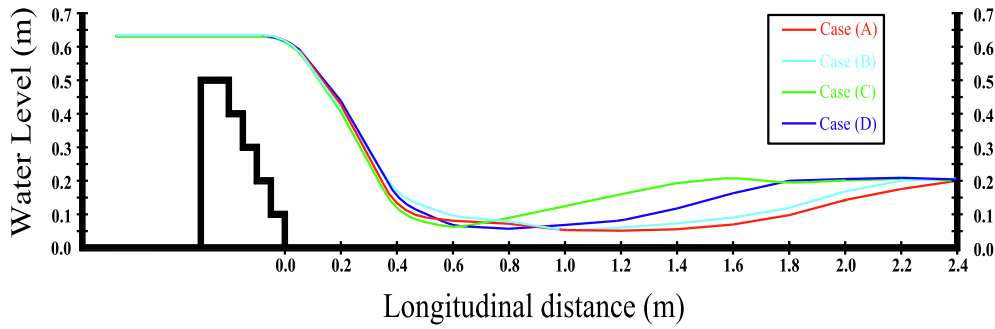
**Fig. 12.** Water Surface Profiles for Different Bed Water Jets Arrangement.
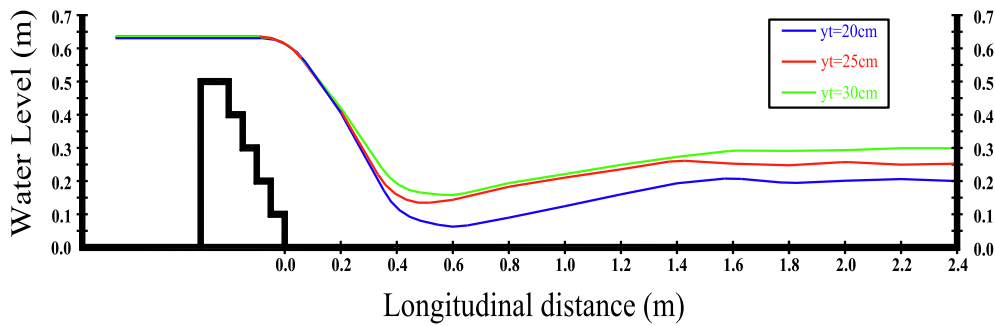


**Fig. 13.** Water Surface Profiles for Different Tailwater Depths and Q = 180 Lit/s; Case (C).

### 4.4. The water surface profiles

Water surface profiles for different bed water jets arrangements are obtained by recording longitudinal water levels for the different tested cases. The observed measurements are presented in Fig. 12 for a total flow discharge, $Q_t$ = 180 Lit/s and tailwater depth, $y_t$ = 20 cm. It can be noticed that the influence of water jets arrangement on the upstream flow depth is non sensible because of the discharge over stepped back weir, $Q_{sw}$ is remained constant. While, case (C) gave the highest flow depth downstream of the hydraulic jump. These findings are in good agreement with the concluded ones earlier in Sections 4.1 and 4.2 that the maximum energy dissipation efficiency and the shortest hydraulic jump are obtained with case (C). The concluded remarks are explained because the bed water jets arrangement in case (C) strike the hydraulic jump at the roller region, and leads to rise of the water level.

To explore the influence of tailwater depth, $y_t$ and total discharge, $Q_t$ on the water surface profile in the presence of bed jets arrangement of case (C); Figs. 13 and 14 are presented. Emphasizing on Fig. 13, it is found that the hydraulic jump length is decreased by the increase of $y_t$. That is resulted in the increase of

the sequent depth, hence the increase of the specific force downstream of the jump which is consistent with Fig. 7 and Table 2. Also, the specific energy associated with the sequent depth is decreased as the flow velocity decreased, consequently the energy dissipation efficiency, η increases, which confirming the findings of Fig. 3.

Fig. 14 demonstrates that the upstream flow depths are increased with the increase of $Q_t$ due to the constant cross section and upstream flow velocity. However, for the downstream flow pattern it is noticed that the jump initial depth, $y_1$ is inversely proportional to the $Q_t$. In contrast, the sequent depth, $y_2$ and the jump length, $L_j$ are increased with $Q_t$, due to the presence of bed water jets. These results are consistent with the outcomes of Fig. 8.

The experimental results are used to develop empirical formulae for estimating the energy dissipation efficiency, **η** and the hydraulic jump characteristics, $\frac{L_j}{y_1}$. By implementing nonlinear regression analysis, the following observational equations are created:

$$\eta = -1.51\left(\frac{Q_j}{Q_t}\right) - 0.01F_{r1} + 0.005\left(\frac{X}{y_1}\right) + 1.11\left(\frac{U_m}{U_1}\right)$$
$$- 0.057 \tag{7}$$
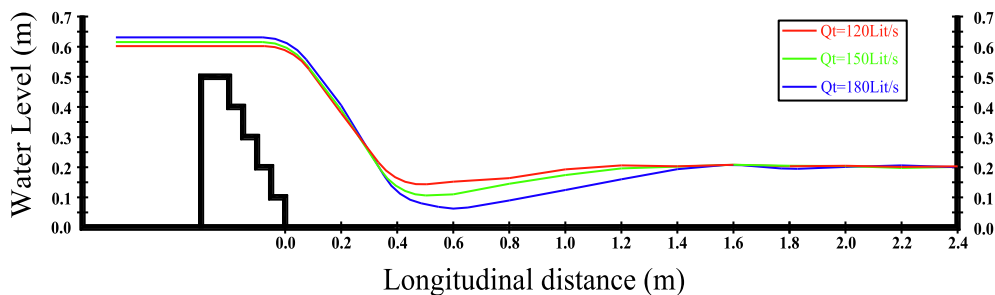


**Fig. 14.** Water Surface Profiles for Different Flow Discharges and $y_t$ = 20 cm; Case (C).

$$\frac{L_j}{y_1} = 17.26\left(\frac{Q_j}{Q_t}\right) + 3.1F_{r1} - 2.95\left(\frac{X}{y_1}\right) - 10.64\left(\frac{U_m}{U_1}\right) + 11.76 \quad (8)$$

The coefficients of determination ($R^2$) for Equations (7) and (8) are 0.766 and 0.838, respectively. The equations are valid for the following conditions: $0 \leq \frac{Q_j}{Q_t} \leq 0.1$; $1.15 \leq F_{r1} \leq 4.99$; $0 \leq \frac{X}{y_1} \leq 98.04$; $0.178 \leq \frac{U_m}{U_1} \leq 0.338$. The derived formulas deduced that the $\frac{Q_j}{Q_t}$ is the dominant variable that influenced the energy dissipation efficiency and the hydraulic jump characteristics. Equation (7) demonstrates that the $\eta$ is inversely related to the $\frac{Q_j}{Q_t}$ and $F_{r1}$ which confirming the givens of Fig. 3. This is due to the fixed jet discharge in the study; $Q_j$ = 12 Lit/s, where the total discharge increases, the term of $\frac{Q_j}{Q_t}$ decreases and the energy dissipation efficiency increases. On the contrary Equation (8) that proved the $\frac{L_j}{y_1}$ is increased as the $\frac{Q_j}{Q_t}$ and $F_{r1}$ increased which agreed with the outcomes of Figs. 5 and 8. Exploring the variable of minor influence on the $\eta$ and $\frac{L_j}{y_1}$; Equations (7) and (8) exhibited that it is recorded at $\frac{X}{y_1}$.

## 5. Conclusions

In the present study, the effect of bed water jets arrangements and the weir stepped back type on the hydraulic jump characteristics including the energy dissipation efficiency, the jump length, the downstream flow velocity distribution in vertical and longitudinal directions and as well the water surface profiles are explored. Based on the results analysis, it can be concluded that the presence of bed water jets regardless of their arrangements significantly enhanced the skimming flow regime in terms of the energy dissipation efficiency and the hydraulic jump characteristics. For the studied flow cases, as the initial Froude number increases, the energy dissipation efficiency is decreased and the hydraulic jump length is increased.

Considering the bed water jets installation, case (C) gives the optimal arrangement where the average energy dissipation efficiencies is increased up to 70.8%, the average jump lengths are decreased up to 48%, the smallest vertical and longitudinal flow velocity distributions downstream of the weir apron toe are recorded as well compared to the non-jetted case.

Regarding the weir back type, the stepped back weir increases the energy dissipation efficiency by about 40% and decreases the hydraulic jump length by about 31% compared to 1:2 sloped back weir for similar flow conditions.

Focusing on the water surface profiles, they are noticeably influenced by different hydraulic characteristics only at the hydraulic jump roller zone.

## 6. Recommendations

For future works, it is recommended to share the outcomes of the current study with electromechanical specialists with significant contribution of project management leaders to explore the adequacy of the presented technique for field application from technical and financial aspects compared to the traditional energy dissipaters methodologies. Examining the methodology of bed water jets downstream stepped back weir with 2H: 1 V step dimensions. Explore the effectiveness of bed water jets downstream different hydraulic structures. Also, check a staggered arrangement of bed water jets, and compare the outcomes with the results of this research.

## Declaration of Competing Interest

The authors declare that they have no known competing financial interests or personal relationships that could have appeared to influence the work reported in this paper.

## References

[1] Hager WH, Bremen R. Bremen, classical hydraulic jump: sequent depths. J. Hydraul. Res. IAHR 1989;27(5):565–85. doi: https://doi.org/10.1080/00221688909499111.

[2] Long D, Steffler P, Rajaratnam N. LDA study of flow structure in submerged hydraulic jump. J. Hydraul. Res. IAHR 1990;28(4):437–60. doi: https://doi.org/10.1080/00221689009499059.

[3] H. Chanson, L. Toombes, Energy Dissipation in Stepped Waterway, the 27th, Proceeding, XXVII IAHR, Congress, 1997, pp. 595–600.

[4] Hossein S, Ehsan J, Reza B, Mehdi A. Discharge coefficient and energy dissipation over stepped spillway under skimming flow regime. KSCE J Civ Eng 2015;19(4):1174–82.

[5] Chanson H. Hydraulic design of stepped spillways and downstream energy dissipaters. Dam Energy J. 2001;11(4):205–42. staff.civil.uq.edu.au/h.chanson/reprints/dameng01.pdf.

[6] Javan M, Eghbalzadeh A. 2D numerical simulation of submerged hydraulic jumps. Appl. Math. Modell. 2013;37(10):6661–9. doi: https://doi.org/10.1016/j.apm.2012.12.016.

[7] Jesudhas V, Roussinova V, Balachandar R, Barron R. Submerged hydraulic jump study using DES. J. Hydraul. Eng. 2016;143(3):04016091. doi: https://doi.org/10.1061/(ASCE)HY.1943-7900.0001231.

[8] Helal E, Fahmy S, Wafaa A. Numerical assessment of the performance of bed water jets in submerged hydraulic jumps. J. Irrig. Drain Eng. 2020;146(7):04020014. doi: https://doi.org/10.1061/(ASCE)IR.1943-4774.0001475.

[9] Peterka A. Hydraulic Design of Stilling Basins and Energy Dissipaters. Engineering Monograph No. 25. 8th ed. Denver: US Bureau of Reclamation; 1984.

[10] Abdelhaleem FSF. Effect of semi-circular baffle blocks on local scour downstream clear-overfall weirs. Ain Shams Eng. J. 2013;4(4):675–84. doi: https://doi.org/10.1016/j.asej.2013.03.003.

[11] Abdel Aal G, Sobeih M, Helal E, El-Fooly M. Improving energy dissipation on stepped spillways using breakers. Ain Shams Eng. J. 2018;9(4):1887–96. doi: https://doi.org/10.1016/j.asej.2017.01.008.

[12] Amany A, Maha R, Nesreen M. Scour characteristics downstream converging spillways. Egypt. Int. J. Eng. Sci. Technol. 2016;19(1):258–66. , https://eijest.journals.ekb.eg/article_97129_11214c3cd45f5c9c1d01e0f0e0f1fdaf.pdf.

[13] I. Ahmed, Using Jets to Minimize the Passive Influence of Hydraulic Jump Downstream Hydraulic Structures (Thesis of PhD), Faculty of Eng. At Shoubra, Benha University, 2020. http://srv5.eulc.edu.eg/eulc_v5/Libraries/Thesis/BrowseThesisPages.aspx?fn=PublicDrawThesis&BibID=12640017.

[14] Zhang G, Chanson H. Air-water flow properties in stepped chutes with modified step and cavity geometries. Int. J. Multiph. Flow 2018;99:423–36. doi: https://doi.org/10.1016/j.ijmultiphaseflow.2017.11.009.

[15] Al-Fawzy A, Al-Mohammed F, Al-Fatlawi J, Al-Zubaidy R. Dissipation energy of flow by stepped type gabion weir. IOP Conf. Ser. Mater. Sci. Eng. 2020;737:. doi: https://doi.org/10.1088/1757-899X/737/1/012158012158.

[16] Chinnarasri C, Donjadee S, Israngkura U. Hydraulic characteristics of gabion-stepped weirs. J. Hydraul. Eng. 2008;134(8):1147–52. doi: https://doi.org/10.1061/(ASCE)0733-9429(2008)134:8(1147).

[17] AlTalib AN, Mohammed AY, Hayawi HA. Hydraulic jump and energy dissipation downstream stepped weir. Flow Meas. Instrum. 2019;69:101616. doi: https://doi.org/10.1016/j.flowmeasinst.2019.101616.

[18] Stefan F, Hubert C. Energy dissipation down a stepped spillway with nonuniform step heights. J. Hydraulic Eng. 2011;137(11). doi: https://doi.org/10.1061/(ASCE)HY.1943-7900.0000455.

[19] Jean G, Bassam R. Stepped spillway as an energy dissipater. Canadian Water Resour. J. 2004;29(3):147–58. doi: https://doi.org/10.4296/cwrj147.

[20] A. Al., O. Yousif, Characterizations of flow over stepped spillways with steps having transverse slopes. In: IOP Conference Series: Earth and Environmental Science, 344, The 5th International Conference on Water Resource and Environment (WRE 2019) 16–19 July, Macao, China. doi:10.1088/1755-1315/344/1/012019.

[21] Li S, Yang J. Effects of inclination angles on stepped chute flows. Appl. Sci. 2020;10(18):6202. doi: https://doi.org/10.3390/app10186202.

[22] Ghaderi A, Abbasi S, Abraham J, Azamathulla HM. Efficiency of trapezoidal labyrinth shaped stepped spillways. Flow Meas. Instrum 2020;72:101711. doi: https://doi.org/10.1016/j.flowmeasinst.2020.101711.

[23] Zongshi D, Junxing W, David F, Robert M, Guangming T. Numerical simulation of air-water two-phase flow on stepped spillways behind X-shaped flaring gate piers under very high unit discharge. Water 2019;11(10):1956. doi: https://doi.org/10.3390/w11101956.

[24] Nikseresht A, Talebbeydokhti N, Rezaei M. (2012) Numerical simulation of two-phase flow on step-pool spillways. Sharif Univ. Technol. 2013;20(2):222–30. doi: https://doi.org/10.1016/j.scient.2012.11.013.